Available online at www.sciencedirect.com

ScienceDirect

journal homepage: www.elsevier.com/locate/he

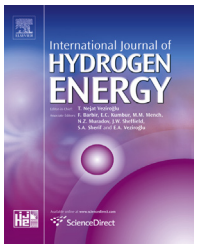

Numerical modeling of hydrogen absorption measurements in Ni-catalyzed Mg

*Federico Cova**, *Fabiana Gennari*, *Pierre Arneodo Larochette*

Consejo Nacional de Investigaciones Científicas y Técnicas, CONICET, Instituto Balseiro (UNCuyo and CNEA), Centro Atómico Bariloche (CNEA), R8402AGP S. C. de Bariloche, Río Negro, Argentina

ARTICLE INFO

Article history:
Received 4 November 2013
Received in revised form
7 January 2014
Accepted 13 January 2014
Available online 15 February 2014

Keywords:
Kinetic model
Magnesium hydride
Hydrogen
Hydrogen storage

ABSTRACT

Magnesium has been deeply studied as a possible hydrogen storage material for both, mobile and static applications. In this work, hydrogen absorption in Ni-catalyzed magnesium was measured in a wide range of pressure (500 kPa–5000 kPa) and temperature (498 K –573 K). Using this information, a model for the absorption kinetics and thermal behavior of the hydrogen storage system was proposed. This model could be used in the design of Ni-catalyzed magnesium storage tanks and other applications. It considers the independent contribution of three variables: temperature, pressure and reacted fraction to estimate the hydrogen absorption rate. An activation energy for the process was estimated and the value obtained (92 kJ/mol) was concordant with previous values reported in the literature.

1. Introduction

One of the most important obstacles in the design of hydrogen-powered vehicles is the lack of safe and efficient hydrogen storage systems for on-board applications. Magnesium is considered a very promising material for hydrogen storage for various reasons: relatively high abundance, low price, high storage capacity (7.6 wt.%) and excellent reversibility [1,2]. However, it has some important drawbacks, in particular the high temperature needed for the hydrogen sorption and the slow reaction kinetics and the difficulty of absorbing the theoretical hydrogen storage capacity of the material.

In order to lower the sorption temperature several studies have been carried out, most of them focused on the use of transition metals and transition metal halides or oxides as additives [3–6]. The main reasons for this choice are the high affinity between transition metals and hydrogen atoms, and their ability to exchange electrons during the reaction (changing their valence and allowing an easier dissociation of the hydrogen molecule as well as the possibility of chemical interaction between the transition metal and the magnesium [3]). These characteristics allow the transition metals and its oxides and halides to strongly improve the kinetic behavior of the magnesium-hydrogen system at low temperature [6]. However, these temperatures are still too high for mobile applications. To enhance the sorption kinetics, it is of great importance to determine the mechanism which governs the reaction rate or the contribution of each step.

Different models and equations have been proposed to predict the kinetic behavior of metal-hydrogen systems and to determine the controlling step of the reaction [7,8]. Flanagan

* *Corresponding author*. Centro Atómico Bariloche (CNEA), R8402AGP S. C. de Bariloche, Río Negro, Argentina. Tel.: +54 294 4445278; fax: +54 294 4445190.
E-mail address: covaf@cab.cnea.gov.ar (F. Cova).

0360-3199/$ – see front matter
http://dx.doi.org/10.1016/j.ijhydene.2014.01.100

et al. [7] proposed various equations for a wide range of reactions, classified in four different subtypes according to the controlling mechanism: nucleation, geometrical contraction, diffusion and reaction-order. Chou [8] proposed a new model for hydrogen absorption in intermetallic systems based on a core–shell structure which could predict the rate limiting step of gas–solid reactions. Both cases present functions which only consider one variable: the reacted fraction [7,8]. Other authors have presented rate equations which depend on the system pressure with several pressure dependence functions [9–11]. Pressure and reacted fraction can be independent or not, according to how the measure was made. These last analyses were specially developed for metal-hydrogen systems and then involve as variable the equilibrium pressure of a hydride phase.

In previous work we could determine that the MgH_2–Ni system presents favorable properties as a hydrogen carrier, showing fast absorption, and a little dependence on temperature on the absorption behavior over 473 K [12]. To identify the factors which determine the reaction rate of the MgH_2–Ni system, a model based on hydrogen absorption measurements is presented in the current paper. A reaction rate function based on three independent contributions (pressure (P), temperature (T) and the reacted fraction (x)) has been considered:

$$r(x,P,T) = f(T)g(P)h(x) \quad (1)$$

The reacted fraction x was calculated as the ratio between the amount of hydrogen absorbed at a given time and the weight of hydrogen absorbed at the end of the reaction.

In order to recognize the variable that mostly influences the hydrogen absorption rate, the behavior of the Ni-catalyzed MgH_2 in a wide range of pressure and temperature was analyzed. The current work is focused on the modeling of hydrogen absorption rather than desorption, for the absorption kinetics is faster and leads to greater thermal differences. This would allow to focus the effort to make the system viable. The final equation provides a quite accurate prediction of the system behavior and could be used to estimate the effect that temperature and hydrogen pressure could have on the reaction rate.

2. Experimental

The samples were prepared by milling a mixture of MgH_2 (Sigma–Aldrich hydrogen storage grade) and Ni (Alfa Aesar powder mesh <300) in a 50:1 molar proportion. The milling was performed for 10 h under Ar atmosphere at 400 rpm with a Fritsch Pulverisette 6 planetary mill with stainless steel vial and balls. A ball/sample weight ratio of 40:1 was used. All the sample manipulation was handled in an Ar-filled glove box equipped with a purification system, in which the typical H_2O/O_2 levels were below 1 ppm.

The absorption kinetics measurements were performed in a Sieverts-like device, with temperatures varying from 423 K to 573 K and an initial pressure range from 500 kPa to 5000 kPa. This range was selected because the vapor pressure of the magnesium is relatively high for temperature over 573 K, restraining its application to temperatures below this limit.

Different sample holders were proposed to minimize the effect of the reaction enthalpy during the absorption. An estimation of the maximum expected raise in temperature was done prior to the selection of the sample holder. Assuming an adiabatic system, and considering the $\Delta H = -70$ kJ/mol of H_2 and a magnesium heat capacity value (C_P) of 29.2 J/mol K [13], the temperature would be increased to more than 2000 K, if the reaction was fully completed. Although this value is much higher than the real one observed during the absorption, it indicates the relevance of the thermal effects that occur in the system. In order to reduce the impact of this effect, the sample holder was designed with a central mass that acts as a buffer absorbing part of the heat released and dissipating it.

The sample holder and its central mass are made of Cu, which- compared to steel- has higher thermal conductivity [13]. Hence, once the sample is in contact with the holder surface a better heat transfer occurs. Taking this Cu mass into account, the temperature increment was recalculated and the new value obtained was lower than 150 K. This holder shows more thermal stability than others. As a reference, the amount of sample used in the experimental measurements was 0.15 g and the weight of the Cu central mass was about 10 g.

Due to the sudden expansion of the hydrogen at the beginning of each experiment and the fast kinetics of absorption reaction it is very difficult to obtain a first measured point without an inherent error. The first measured pressure could be different from the real one. To correct this effect, all absorption curves were processed adjusting the first point so that the final capacity of the absorption matches the capacity of the subsequent experiment of hydrogen desorption.

The temperature was measured outside the reactor. Fig. 1 shows a scheme of the device, indicating the spot in which the thermocouple is located. It is possible to notice that a stainless steel wall separates the sample holder from the thermocouple as it is usual in these devices. This configuration is the most common and the simplest to scale up to a storage tank. For this reason is important to be able to predict the thermal behavior of the system based in the outside temperature.

The thermocouple was calibrated for stationary conditions, which allows to know accurately the initial temperature inside the reactor. However, measured and sample temperatures could be significantly different as the reaction proceeds. Therefore, the variation of the temperature measured is not an accurate representation of the variations that occur in the sample. Considering the values calculated previously, the system was not considered isothermal, and the following heat dissipation equation was used for the thermal behavior:

$$\frac{dT}{dt} = \left(\frac{\Delta H}{C_P}\frac{dx}{dt} - k_T(T - T_{SP})\right) \quad (2)$$

in which k_T is a dissipation factor and T_{SP} is the temperature outside the reactor. This equation considers the heat produced by the reaction inside the sample holder and the heat dissipated through the reactor walls. The simulation of the curves was done with an Euler method for both, the reacted fraction and the thermal equations.

A genetic algorithm was used as a parameter adjusting method. This algorithm takes at random a population of possible parameters and evaluates its goodness of fit. Then it creates a new generation of parameters by mixing the ones

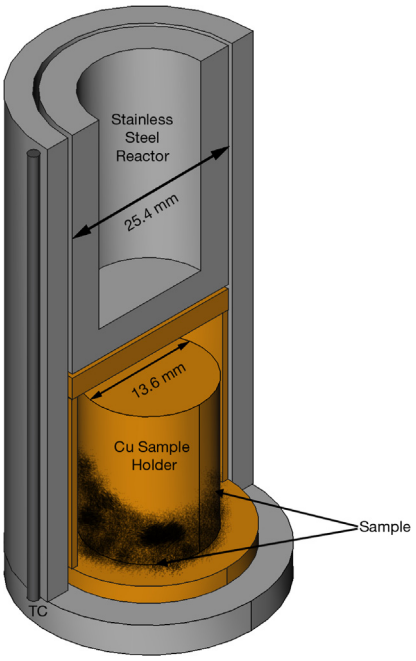

Fig. 1 – Reactor, sample holder and thermocouple location (TC) scheme.

which best fitted the previous generation. In this way, with each generation, the population "evolves" to better results. In this case, an initial population of 200 individuals was selected and it evolved for 30 generations.

3. Results

3.1. *Hydrogen absorption kinetics of Ni-catalyzed MgH_2 samples*

Hydrogen reaction kinetics of the samples was studied by continuous cycling in the Sieverts device. The samples showed an absorption capacity of 5.4 wt.% and high stability after more than 40 cycles of hydrogen absorption/desorption as shown in Fig. 2A. This reduced capacity respect to the theoretical one (7.6 wt.%) is obtained due to the difficult of accessing to the core of the magnesium particles in a reasonable absorption time. In our previous work [12], an XRD analysis of the cycled samples has been presented and the only phases present in the sample were MgH_2 and small amounts of Mg_2NiH_4/Mg_2Ni. No MgO or other compounds have been observed in the studied samples. These results from XRD analysis evidence that the studied material is magnesium hydride, and the Ni composites act as catalysts.

Some of these absorption curves corresponding to different temperatures are shown in Fig. 2B. In all curves the reaction was almost completed in less than 30 s (obtaining a conversion fraction of 0.9). The initial pressure of the system for all the absorption reactions in the figure was 3500 kPa. As expected, the reaction is slightly faster at higher temperatures.

To obtain the dependence (on temperature and pressure) of the reaction rate, the measurements were done in a wide range of pressure (500 kPa–5000 kPa) and temperature (423 K–573 K). From this set of hydrogen absorption curves, the reaction rate was calculated. Considering that the difference between the curves is minor and for a better study of the system, the reaction rate for every data point in the measurements was calculated by a finite difference method, using the slope of the secant between the two closest points (the previous and the following).

Fig. 3 shows the calculated reaction rate at different pressures and temperatures, at a converted fraction of 0.5. Some measurements performed at intermediate temperatures are not shown in the figure. The points in the figure represent the average reaction rate of the measurements performed under the referred conditions. All the data point includes the reaction rate calculated from 5 to 10 absorption measurements each. The high temperature absorption curves (>468 K) in Fig. 3 seem to overlap. The low temperature curves (<438 K) also overlap with each other but not with the high temperature curves. It is noticeable that in the intermediate temperature curves (438 K–468 K) the samples present a dual behavior: at low pressure the rate is similar to the low temperature rates, but at higher pressure the rate is closer to the

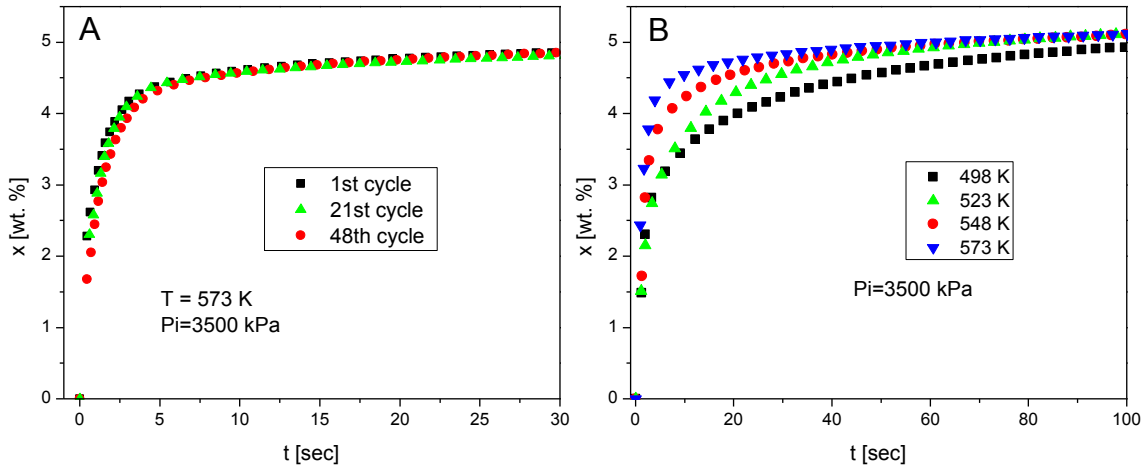

Fig. 2 – Hydrogen absorption curves of the Ni-catalyzed magnesium samples after a different number of cycles (A) and at different temperatures (B).

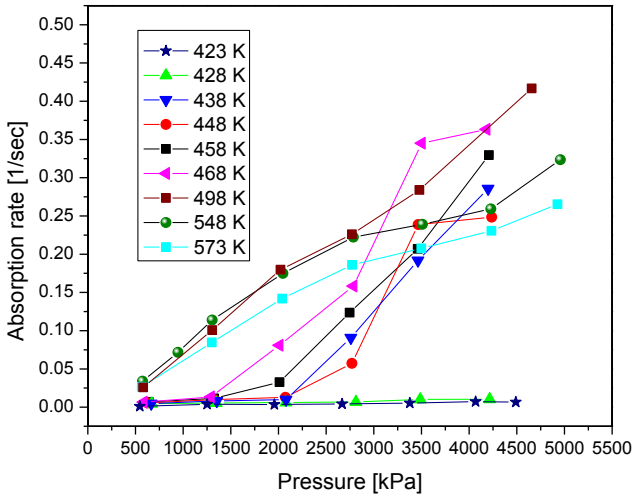

Fig. 3 – Hydrogen absorption rates against system pressure at different temperatures.

high temperature rate. This strongly indicates that a different mechanism controls the low and high pressure absorption reaction for intermediate temperatures.

To analyze the variation of the driving force of the reaction at each temperature, the reaction rates were plotted against a reduced pressure, defined as the ratio between the actual pressure of the system and the equilibrium pressure ($P_{red} = P/P_{eq}$). The hydrogen absorption rate as a function of the reduced pressure at different temperatures is shown in Figure A1 from the supplementary material. It is also possible to see the temperature dependence of the system even at high temperatures, but it is still possible to note that some of the curves show the previously mentioned dual behavior.

In the current work the absorption reaction in all the range of pressures and high temperatures is studied and modeled with Equation (1). The study of absorption reactions at low pressure and temperature will be presented in a future article. Due to the methodology of the experiments these variables are not strictly independent; x and P are tied by the volume of the Sieverts device and the weight of the sample. Besides, P_{eq} is a function of temperature, as described in the Van't Hoff equation. However, as the aim of the current work is to determine a general equation to describe the behavior of the system in different conditions, these three variables have been separated and treated independently. From Equation (1), the rate equation can be expressed as follows:

$$r\left(T, \frac{P}{P_{eq}}, x\right) = R.f(T)g\left(\frac{P}{P_{eq}}\right)h(x) \quad (3)$$

Equation 3 shows the dependence of the reaction rate on the three mentioned variables: the temperature dependence (f), the effects of the driving force (g), and the influence of the reacted fraction (h). R is a parameter to be determined in the simulation of the absorption kinetics.

For the analysis, two of the variables were set at constant values and the absorption rate was calculated for different values of the third variable. Then, a fitted function was tried out, which should be the independent equation of the corresponding variable.

3.2. Temperature dependence

For the temperature dependence an Arrhenius-like equation was proposed:

$$r(T) = F \cdot A e^{-\frac{E}{R_g T}} \quad (4)$$

in which R_g is the gas-law constant, A is a pre-exponential factor, E is the activation energy of the process and F is the contribution of the other two equations to the reaction rate.

The result of the fitting for a reduced pressure value of 20 and a reacted fraction value of 0.5 is shown in Fig. 4. The fitting is not very accurate in the high temperature data points. This happens because the temperatures considered were assumed as the initial temperature; however, these values will be corrected with the results obtained from the temperature variation simulations. The activation energy obtained was 121 kJ/mol H_2.

3.3. Reacted fraction dependence

Fig. 5A and B presents the absorption rate dependence on the reacted fraction for four different temperatures at reduced pressure equal to 20 (Figure 5A) and 30 (Fig. 5B). The simplest function to fit the data was a linear model. While this model could be considered a good approximation because it allowed the fitting for the values in the 0.25–0.75 range, it was unable to reproduce the experimental data for reacted fractions close to 1 because it reached a value of 0 at a converted value of 0.8. Therefore, a new data point corresponding to converted fraction equal to 1 and a reaction rate value of 0 was added, and an equation which fulfills this condition was proposed:

$$r(x) = H\frac{1-x}{b+x} \quad (5)$$

In Equation (5), H is a constant which takes into account the product between $f(T)$ and $g(P_{red})$ (see Equation (3)); and b is an

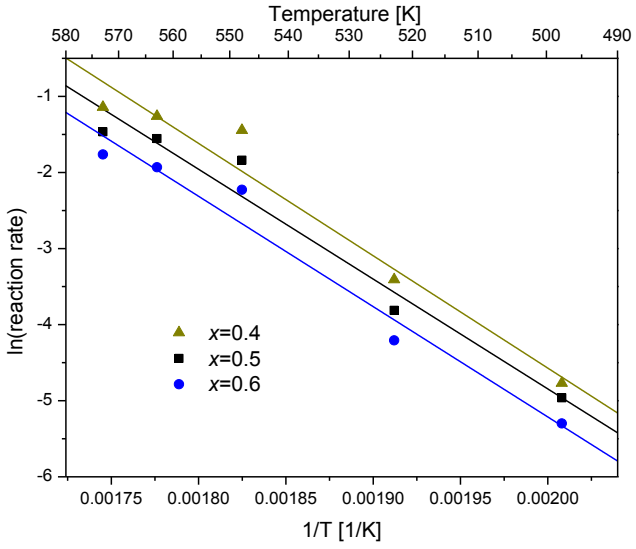

Fig. 4 – Hydrogen absorption rates against temperature at reduced pressure equal to 20 and converted fraction values of 0.4, 0.5 and 0.6.

adjustable parameter which defines the shape of the curve. This equation has its maximum value for converted fraction equal to zero and a minimum value of 0 when the reaction is completed. This function behaves linearly for lower values of x, and its slope decreases with increasing values of x.

The parameters have been adjusted for the curves in Fig. 5A and B. Parameter b was very similar for every fitted curve; an average (0.36) of all values was made. This value of 0.36 was adopted for the subsequent recalculations of the parameter H.

3.4. Pressure dependence

The last needed function is $g(P_{red})$, which considers the influence of the driving force depending on the pressure. The absorption rate as a function of the reduced pressure for three different temperatures is presented in Fig. 6A–C; a linear fit has been used. The selected function was:

$$r(P_{red}) = G\cdot(P_{red} - 1) \quad (6)$$

G is a parameter to be fitted which includes the value of the other two functions (Fig. 6D). This equation ensures that when the driving force is zero, the rate will also be zero. These rates were calculated for a reacted fraction of 0.5.

This model is not very accurate to describe the data points, but it has to be reevaluated after the temperature corrections are made.

3.5. General equation

Once the three independent functions were obtained, $f(T)$, $g(P_{red})$ and $h(x)$, it was possible to propose a general expression of the reaction rate as a function of P_{red}, T and x:

$$r\left(T, \frac{P}{P_{eq}}, x\right) = R\cdot\left(\frac{P}{P_{eq}} - 1\right)\frac{1-x}{b+x}Ae^{-\frac{E}{RgT}} \quad (7)$$

The parameter R includes the parameters F, G and H.

In order to use this equation for modeling absorption curves like those shown in Fig. 2B, it is necessary to consider the thermodynamics of the system. Due to the high reaction enthalpy and the fast kinetics of the absorption reaction, the increase of the sample temperature which influences the reaction rate, is a major factor to be taken into account. To introduce this thermal behavior of the system, a simple equation has been proposed to model the temperature changes during the absorption reaction (Equation (2)).

A genetic algorithm was used to determine the value of the parameters R and k_T.

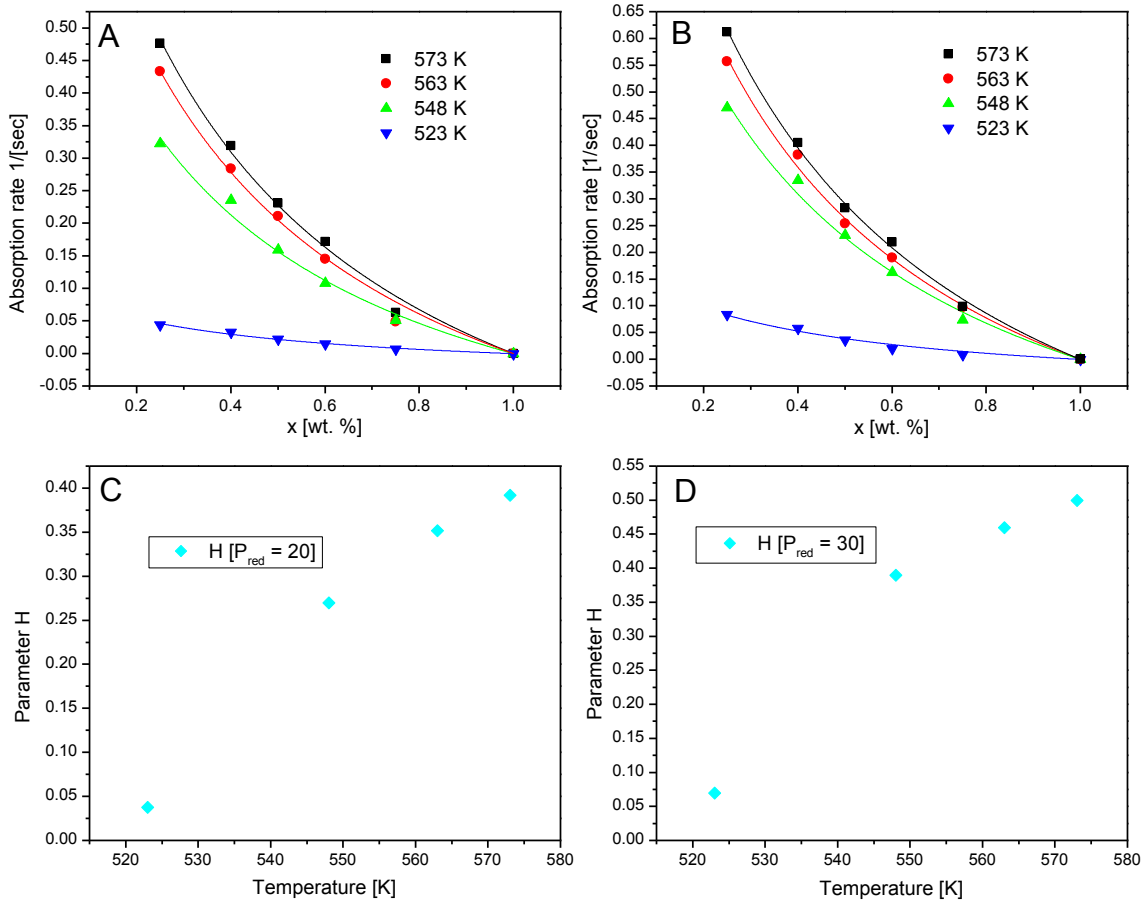

Fig. 5 – Hydrogen absorption rates against converted fraction at a reduced pressure equal to 20 (A) and reduced pressure equal to 30 (B); and the corresponding variation of the H parameter with the temperature (C and D).

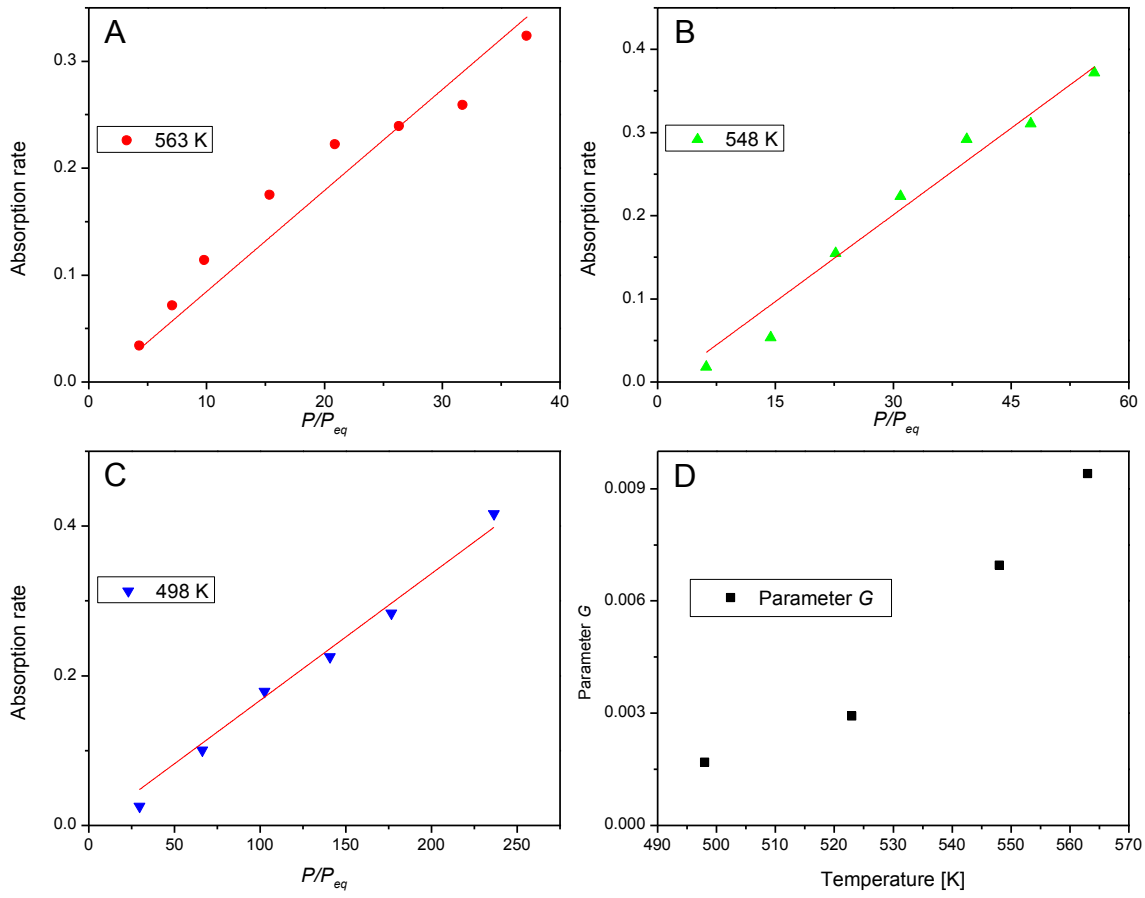

Fig. 6 – Hydrogen absorption rates against reduced pressure for different temperatures (A, B and C) at a converted fraction of 0.5; and the variation of the equation parameter with the temperature (D).

The data range used for the simulation was from 0 to 0.8 of the reacted fraction. The curves simulated were compared with an average experimental curve for each temperature-initial pressure pair, obtained from 5 to 10 independent measured curves. The criterion used to determine the optimum value of the parameters was the average squared difference between the calculated pressure value and the experimental value in the considered range.

All the simulated curves showed a maximum deviation lower than 5% and an average squared deviation between 0.5% and 3% in the range of interest. This indicates that the model provides a reliable approximation to the experimental data in a range of reacted fraction between 0 and 0.8. The value of parameter *R* resulted to be different from one simulation to the other, varying between 0.76 and 5.17. This can be attributed to the inaccurate activation energy calculated considering the wrong temperatures.

With the simulated pressures and temperatures it was possible to obtain a plot of the reaction rate against the real-time reduced pressure calculated with the temperature obtained with the simulation. Using this information the values in the Fig. 3 were recalculated and new values for the Arrhenius parameters were obtained. These results are shown in Fig. 7. The linear fit in Fig. 7 gives an activation energy value for the process of 81 kJ/mol of H_2. This value is reasonable for this kind of process and catalyzed-material [14–17].

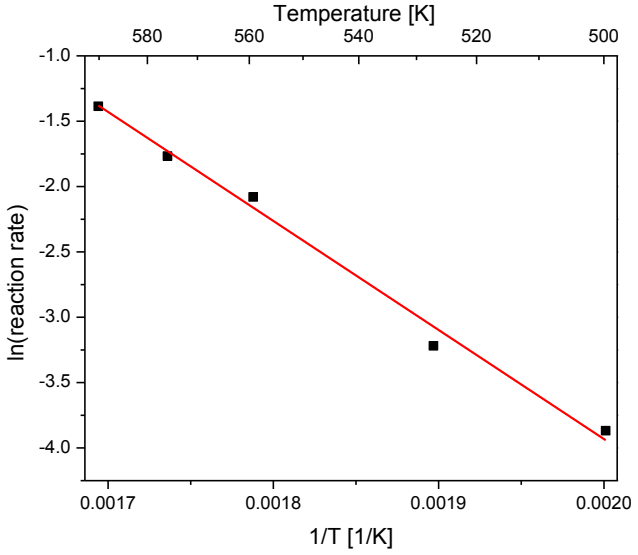

Fig. 7 – Logarithm of the reaction rate against the inverse of the temperature at a reduced pressure of 12.5 and a reacted fraction of 0.5.

Due to the new knowledge about the system temperature evolution, Fig. 6 is not a very good representation of the reaction rate dependence with the reduced pressure. In Figure A2 from complementary material the reaction rate is plotted against the corrected reduced pressure. It is possible to notice that the linear model is more accurate when the corrections are made.

Fig. 8 summarizes the absorption reaction rate dependence with different variables. From this figure it is deduced that pressure is the main factor in the increment of temperature during the reaction. At higher pressures the raise of temperature is also more significant (Fig. 8D and H). Still, an increment in the initial temperature shows a lesser impact in the thermal behavior of the system (Fig. 8B and F). The second point of each curve is the one that differs most from the fitting. This could be ascribed to the difficulty in measuring the pressure after the sudden expansion at the beginning of the experiment. In this new simulation the parameter *R* varied in a more limited range (0.88–1.32 for a temperature range between 523 K and 573 K). The values adjusted for 498 K varied from 1.8 to 3.9, which could indicate that a transition mechanism is controlling the reaction at this temperature. The variations in temperature observed during the whole reaction confirm that this reaction did not occur under isothermal conditions.

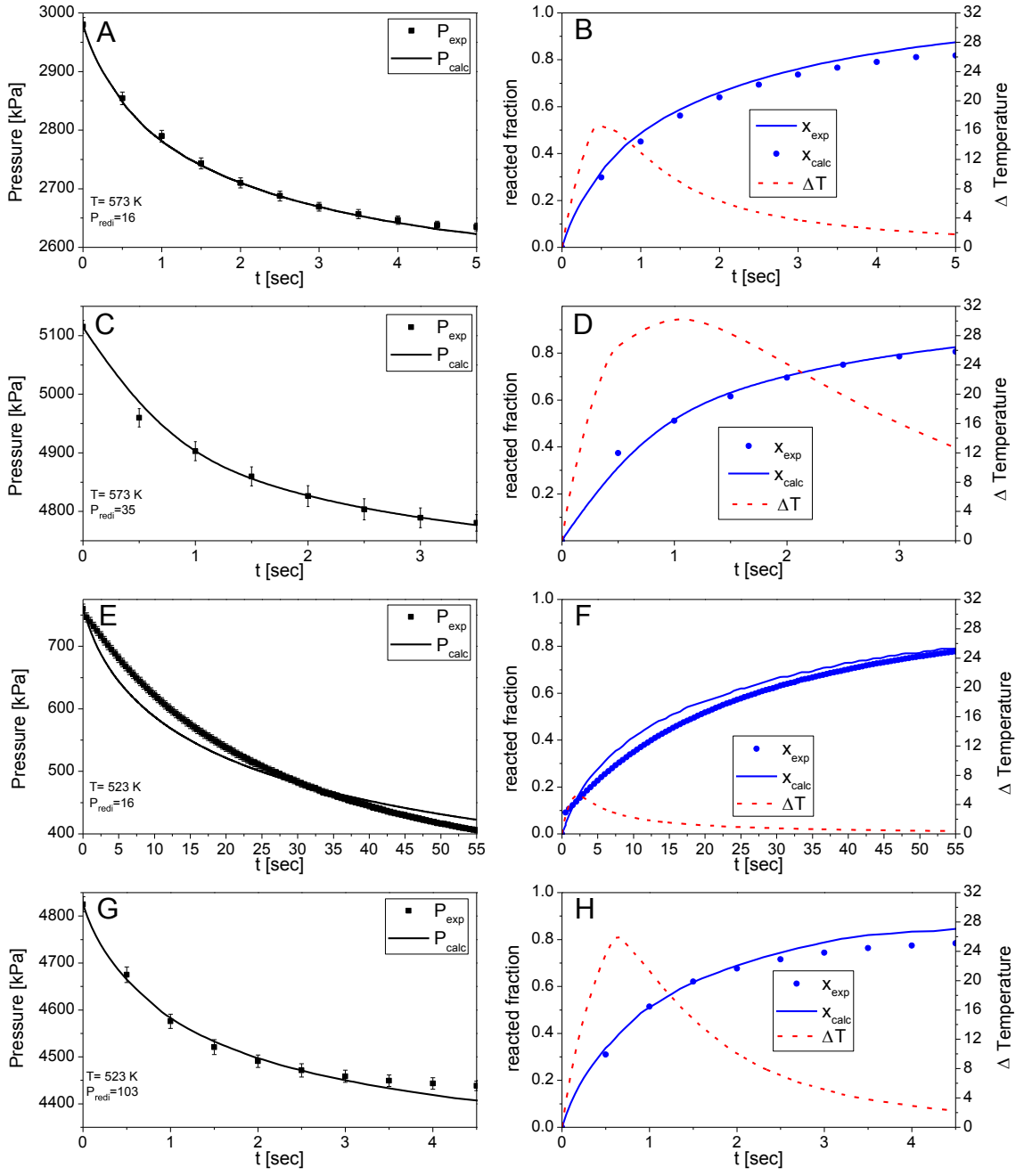

Fig. 8 – Simulated curves (full line) and experimental data (scatter points) of: Pressure (A, C, E, G) and reacted fraction (B, D, F, H) as a function of time. The calculated temperature variation (dashed line) is shown in B, D, F, H.

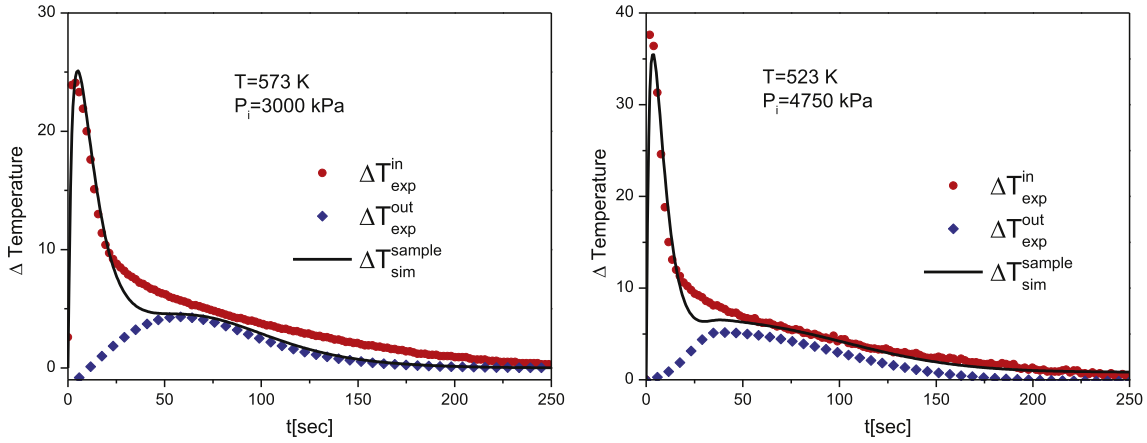

Fig. 9 – Simulated curves (full line) of the sample temperature variation with time and experimental data (scatter points) of the temperature evolution, inside and outside the reactor.

With these new curves, the reaction rate was plotted against temperature for a constant value of reduced pressure. These results were fitted with an Arrhenius curve and the new activation energy value (92 kJ/mol of H_2) was very close to the value previously obtained. Therefore, another step in this iterative process was considered unnecessary.

In an attempt to assess the predictive power of the model proposed for the system temperature, some of the measurements were reproduced in a similar Sieverts device with a thermocouple placed in contact with the sample. The comparison between the measured data and the simulated is shown in Fig. 9. The agreement between these values is very good. This is a validation of the model developed in the current work, allowing its application in other similar systems.

4. Conclusions

In this work the hydrogen absorption in Ni-catalyzed magnesium was studied in a wide range of both, temperature and pressure. The reaction rate evolution with time was calculated for every measurement. The analysis of this reaction rate showed two different behaviors of the system under different reaction conditions. The high temperature behavior has been studied and a new model for the hydrogen absorption kinetics has been proposed. The low temperature measurements will be studied in a future article.

This new model presents a range of activation energies based in the initial considerations. The energy values obtained are concordant with the reported in previous works. The different activation energies calculated were all concordant with the reported data. It allows to conclude that the assumptions done during the measurements and calculations can lead to different values of the activation energy for the same system. This is an important result to understand the variation in the values presented in the literature.

Different functions were obtained for the dependence of the reaction rate on the considered variables (pressure, temperature and reacted fraction), while the other variables were kept constant. With these functions, a new global kinetic function has been proposed for the hydrogen absorption kinetics. The proposed kinetic expressions reproduce quite accurately the experimental data obtained from the volumetric measurements. Furthermore, they allow to consider the temperature variation during the reaction, which is of major importance since most models presented in the literature disregard the temperature variation caused by the reaction. A Fourier-like equation has been proposed for the heat dissipation. This equation was a good estimation for the thermal behavior of the system. The predicted temperature variation of the system was confirmed with the experimental measurements.

The results showed that the thermal effects present in the absorption are significant and should not be neglected. Recent work shows the variation in the volumetric measurements done in different laboratories [18]. This variation might be related to the strong influence of the different thermal behavior of different measuring systems.

Acknowledgments

This study has been partially supported by CONICET (National Council of Scientific and Technological Research), CNEA (National Commission of Atomic Energy), ANPCyT (PICT N° 1049) and Instituto Balseiro (University of Cuyo).

Appendix A. Supplementary data

Supplementary data related to this article can be found at http://dx.doi.org/10.1016/j.ijhydene.2014.01.100.

REFERENCES

[1] Walker G. Solid-state hydrogen storage: materials and chemistry. England: Woodhead Publishing Limited; 2008.
[2] Züttel A, Borgschulte A, Schlapbach L. Hydrogen as a future energy carrier. Switzerland: Wiley-VCH; 2008.

[3] Barkhordarian G, Klassen T, Bormann R. Catalytic mechanism of transition-metal compounds on Mg hydrogen sorption reaction. J Phys Chem B 2006;110:11020–4.
[4] Liang G, Huot J, Boily S, Van Neste A, Schulz R. Catalytic effect of transition metals on hydrogen sorption in nanocrystalline ball milled MgH_2-Tm (Tm = Ti, V, Mn, Fe and Ni) systems. J Alloys Compd 1999;292:247–52.
[5] Jensen TR, Andreasen A, Vegge T, Andreasen JW, Stahl K, Nielsen MM, et al. Dehydrogenation kinetics of pure and nickel-doped magnesium hydride investigated by in situ time-resolved powder X-ray diffraction. Int J Hydrogen Energy 2006;31(14):2052–62.
[6] Ma LP, Wang P, Cheng HM. Hydrogen sorption kinetics of MgH_2 catalyzed with titanium compounds. Int J Hydrogen Energy 2010;35(7):3046–50.
[7] Khawam A, Flanagan DR. Complementary use of model free and modelistic methods in the analysis of solid state kinetics. J Phys Chem B 2005;109:100073–80.
[8] Chou KC, Xu K. A new model for hydriding and dehydriding reactions in intermetallics. Intermetallics 2007;15(5–6):767–77.
[9] Ron M. The normalized pressure dependence method for the evaluation of kinetic rates of metal hydride formation/decomposition. J Alloys Compd 1999;283:178–91.
[10] Martin M, Gommel C, Borkhart C, Fromm E. Absorption and desorption kinetics of hydrogen storage alloys. J Alloys Compd 1996;238(1–2):193–201.
[11] Førde T, Maehlen JP, Yartys VA, Lototsky MV, Uchida H. Influence of intrinsic hydrogenation/dehydrogenation kinetics on the dynamic behavior of metal hydrides: a semi-empirical model and its verification. Int J Hydrogen Energy 2007;32(8):1041–9.
[12] Cova F, Arneodo Larochette P, Gennari F. Hydrogen sorption in MgH_2-based composites: the role of Ni and $LiBH_4$ additives. Int J Hydrogen Energy 2012;37(20):15210–9.
[13] Perry RH, Green DW. Perry's chemical engineers' handbook. 6th ed. New York: McGraw-Hill; 1984.
[14] Kojima Y, Kawai Y, Haga T. Magnesium-based nano-composite materials for hydrogen storage. J Alloys Compd 2006;424:294–8.
[15] Mao JF, Guo ZP, Yu X, Liu H, Wu Z, Ni J. Enhanced hydrogen sorption properties of Ni and Co-catalyzed MgH_2. Int J Hydrogen Energy 2010;35(10):4569–75.
[16] Cabo M, Garroni S, Pellicer E, Milanese C, Girella A, Marini A, et al. Hydrogen sorption performance of MgH_2 doped with mesoporous nickel- and cobalt-based oxides. Int J Hydrogen Energy 2011;35(9):5400–10.
[17] Varin RA, Czujko T, Wronski ZS. Nanomaterials for solid state hydrogen storage. 1st ed. New York: Springer; 2009.
[18] Moretto P, Zlotea C, Dolci F, Amieiro A, Bobet JL, Borgschulte A, et al. A round robin test exercise on hydrogen absorption/desorption properties of a magnesium hydride based material. Int J Hydrogen Energy 2013;38:6704–17.